





Article

Joint User Association and Power Control in UAV Network: A Graph Theoretic Approach

Mohammad Alnakhli ¹, Ehab Mahmoud Mohamed ^{1,*}, Wazie M. Abdulkawi ¹ and Sherief Hashima ^{2,3}

¹ Department of Electrical Engineering, College of Engineering in Wadi Addawasir, Prince Sattam Bin Abdulaziz University, Wadi Addawasir 11991, Saudi Arabia; m.alnakhli@psau.edu.sa (M.A.); w.alkadri@psau.edu.sa (W.M.A.)

² Computational Learning Theory Team, RIKEN-Advanced Intelligence Project (AIP), Fukuoka 819-0395, Japan; sherief.hashima@riken.jp

³ Engineering Department, NRC, Egyptian Atomic Energy Authority, Cairo 13759, Egypt

* Correspondence: ehab_mahmoud@aswu.edu.eg

Abstract: Unmanned aerial vehicles (UAVs) have recently been widely employed as effective wireless platforms for aiding users in various situations, particularly in hard-to-reach scenarios like post-disaster relief efforts. This study employs multiple UAVs to cover users in overlapping locations, necessitating the optimization of UAV-user association to maximize the spectral and energy efficiency of the UAV network. Hence, a connected bipartite graph is formed between UAVs and users using graph theory to accomplish this goal. Then, a maximum weighted matching-based maximum flow (MwMaxFlow) optimization approach is proposed to achieve the maximum data rate given users' demands and the UAVs' maximum capacities. Additionally, power control is applied using the M -matrix theory to optimize users' transmit powers and improve their energy efficiency. The proposed strategy is evaluated and compared with other benchmark schemes through numerical simulations. The simulation outcomes indicate that the proposed approach balances spectral efficiency and energy consumption, rendering it suitable for various UAV wireless applications, including emergency response, surveillance, and post-disaster management.

Keywords: energy efficiency; spectral efficiency; unmanned aerial vehicles (UAV); bipartite graph maximum flow; M -matrix theory



Citation: Alnakhli, M.; Mohamed, E.M.; Abdulkawi, W.M.; Hashima, S. Joint User Association and Power Control in UAV Network: A Graph Theoretic Approach. *Electronics* **2024**, *13*, 779. <https://doi.org/10.3390/electronics13040779>

Academic Editor: Carlos Tavares Calafate

Received: 6 December 2023

Revised: 7 February 2024

Accepted: 14 February 2024

Published: 16 February 2024



Copyright: © 2024 by the authors. Licensee MDPI, Basel, Switzerland. This article is an open access article distributed under the terms and conditions of the Creative Commons Attribution (CC BY) license (<https://creativecommons.org/licenses/by/4.0/>).

1. Introduction

Unmanned aerial vehicles (UAVs) offer several advantages over traditional manned aircraft, making them an attractive solution for various applications such as agriculture, construction, infrastructure inspection, environmental monitoring, and post-disaster response [1–3]. In hard-to-reach scenarios like a post-disaster one, wireless communication systems encounter several challenges including the limiting of available resources due to the destruction/malfunction of the existing wireless infrastructure, which can lead to reduced data rates and limited coverage, posing challenges in reaching impacted communities. Additionally, obstacles and barriers such as debris at disaster sites can disrupt wireless signals, impeding the maintenance of stable connections. Moreover, power supply disruptions during disasters affect the operation of wireless communication devices, restricting their effectiveness in providing essential information and support. Moreover, the complexity of relief efforts involving multiple organizations and agencies introduces coordination challenges, making communication among them difficult and time-consuming. In this tough situation, UAVs can access remote or hazardous areas, rapidly collect data, and perform tasks that would be time-consuming for humans. They can have advanced sensors and imaging technologies, enabling high-precision data collection, mapping, and analysis [4]. Moreover, they are increasingly recognized for their cost-effectiveness, accessibility, efficiency, precision, environmental benefits, and potential for use in various industries [5–8].

In wireless communications, UAVs are being explored to provide wireless connectivity in remote or underserved areas where conventional cellular coverage is limited or unavailable, making them a key enabler of wireless communications [9]. UAVs are also being used in the Internet of robotic things (IoRT), where they can be integrated with sensors, actuators, and other devices to create a network of robotic systems that can perform tasks autonomously [10]. Also, secure vehicular edge computing can be supported using non-orthogonal multiple access (NOMA) as given in [11]. However, due to the growing number of users' demands and their limited battery capacities, efficient spectral and energy optimizations are critical for UAV networks [12]. Thus, the UAV-user association problem, which involves assigning users to appropriate UAVs, is of significant importance as it directly impacts the system's performance, efficiency, and quality of service (QoS) [13]. This is because linking user equipment (UE) to its optimal UAV based on its achievable data rates relative to users' traffic demands in multi-UAV scenarios results in improving the spectral efficiency of the overall network. Additionally, UE transmit powers can be optimized based on these tuned data rates to reduce energy consumption. Compared with the ordinary user association problem, the UAV-user association problem is more challenging due to the dynamic nature of UAVs in the 3D space, resulting in highly overlapping UAV coverage areas [14]. These challenges require innovative algorithms, protocols, and strategies to efficiently handle the UAVs' dynamic 3D airspace communication [14]. Consequently, addressing the UAV-user association problem becomes crucial for maximizing system performance, capacity, and reliability for enabling various UAV applications [13]. The existing literature of UAV association and UE power control [2,15–24] have a critical research gap: most of them did not consider the UE's traffic demands while associating it with the most appropriate UAVs. Also, they never considered the critical point of the UE's limited battery budget through proposing efficient power control schemes as extensively discussed in the related works section in this paper.

To fill in the aforementioned research gap, this paper uses graph theory, specifically the bipartite graph theory, to address the UAV-user association problem while taking users' traffic demands into consideration. Moreover, UE's power control is performed using the efficient M -matrix theory. Generally speaking, graph theory, a mathematical branch studying the properties and relationships of objects represented as nodes and edges in a graph, has wide applications in various fields of wireless communication [25]. Due to its ability to model complex relationships and interactions in a structured and visual manner, graph theory is well-suited for addressing the UAV-user association problem, as will be presented in this paper. This is because it visually represents spatial relationships between UAVs and users in a 3D airspace. In this regard, a bipartite graph is used to model UAV-UE associations, as they represent two different kinds of nodes. Consequently, graph-based optimization algorithms can be used to optimize association decisions and maximize the total network flow. Maximum flow (MaxFlow) is a well-known methodology for maximizing the flow in a graph by optimizing the flows in its associated edges. However, only using the ordinary MaxFlow algorithm to solve the UAV-user association problem and maximizing the network flow delivers poor performance when dealing with dense graphs. Additionally, the classical MaxFlow algorithm may give unacceptable solutions of associating a user with multiple UAVs simultaneously. Therefore, using an alternative approach, such as the maximum weighted matching (MWM) algorithm, to handle the association problem within its constraints before maximizing the network flow using the MaxFlow algorithm will be beneficial. Thus, in this paper, a combination of MWM and MaxFlow algorithms, namely a maximum weighted matching-based maximum flow (MwMaxFlow) optimization approach, will be proposed to handle UAV-user association as well as maximize the network flow given users' demands and UAVs' maximum capacities.

Power control in communication systems, explicitly regulating the transmit powers of UE, is crucial for optimizing system performance in terms of interference management, signal quality, and resource utilization while considering the UE's limited battery capacities [26]. In this regard, the M -matrix theory, known for its optimality, flexibility,

robustness, convergence, scalability, and computational efficiency, is considered a highly effective method for power control in such scenarios [26]. With its ability to model diverse system configurations, the M -matrix theory will optimize the UE's transmit powers while maintaining the minimum link qualities [27]. It is worth mentioning that this paper focuses solely on optimizing the UE's energy consumption while disregarding UAVs' energy consumption. This is due to two main reasons; firstly, the primary factor depleting UAV power is the act of flying and maneuvering, which falls outside the scope of this paper, as our focus is mainly on communication-related issues. Secondly, the power of the UE is considered more critical compared with UAVs due to the challenges involved in recharging UE batteries, particularly in scenarios where the infrastructure is severely damaged after a disaster. Nevertheless, our future investigations will be motivated by the goal of optimizing the energy consumption of UAVs as well.

The main contributions of this paper can be summarized as follows:

- The UAV-user aerial network will be considered to handle the UAV-user association problem by jointly optimizing its spectral and energy efficiencies, especially in post-disaster relief scenarios.
- Toward that, we will utilize the concept of graph theory, specifically the bipartite graph theory, and propose the MwMaxFlow approach to address it. In this approach, the MWM algorithm maximizes the data rates among UAV users by matching (i.e., associating) users to UAVs based on their achievable data rates relative to their traffic demands. Then, the MaxFlow algorithm is utilized to maximize the flow of the whole network constrained by the maximum capacities of UAVs.
- Based on the UAV-user association created in the first step, the UE's transmit powers are optimized using the M -matrix theory to reduce the UE's energy consumption while maintaining the minimum data flow optimized by the MwMaxFlow algorithm. Overall, the two proposed schemes, i.e., the MwMaxFlow-based UAV-user association and the M -matrix theory-based UE power control, maximize both the spectral and energy efficiencies of the UAV-user network while considering users' traffic demands and UAVs' maximum capacities.
- Simulation results demonstrate the effectiveness of the proposed solutions, showing significant improvements in spectral and energy efficiencies compared with other benchmarks. Specifically, the proposed MwMaxFlow achieves a 90% improvement in spectral efficiency compared with the ordinary MaxFlow algorithm in some scenarios. The proposed approach also achieves the highest energy efficiency among the compared benchmark schemes.

The remaining sections of this paper are organized as follows. Section 2 summarizes the related works. Section 3 presents the system model and formulates the problem. Section 4 presents the proposed spectral and energy efficiency optimization approach. Section 5 discusses the results and provides a detailed discussion of the findings. Finally, the limitations of the proposed approach and conclusions summarizing the essential findings and implications of the proposed approach are presented in Sections 6 and 7, respectively.

2. Related Work

Recently, a significant amount of literature has become available on the application of UAVs in wireless communication networks. Some research papers provided a comprehensive survey of resource management in UAV-assisted wireless networks [28], while others focused on energy optimization techniques in UAV-assisted wireless networks. UAVs' flexibility and on-demand deployment make them a promising platform in wireless communication networks [29]. Also, some research studies focused on UAV deployment and trajectory planning in wireless communication networks to minimize both UAV energy consumption and mission completion time [15]. These studies provided insights into the challenges and opportunities of using UAVs in future 6G wireless communication networks and demonstrated the potential of UAVs in improving network performance and enabling new applications. Regarding the main focus of this paper, which is UAV-user association

and user power control, some research works have studied these topics. In [16], the joint placement of UAVs and user association under different constraints to optimize network performance were addressed. However, it did not explicitly discuss energy efficiency, including users' power control. In [17], a reinforcement learning (RL)-based algorithm was proposed to prioritize user association in UAV-assisted emergency communication networks for maximizing the sum rate of the network. One potential shortcoming of this work is the lack of consideration of energy efficiency, which may not be sustainable for battery-powered UE. In [18], a joint optimization algorithm for user association and UAV location in UAV-aided communication networks was studied. One potential shortcoming of this work is that it does not prioritize energy efficiency as a primary optimization objective. Additionally, the algorithm's scalability may be limited, as the genetic algorithm used in the second stage of the algorithm can become computationally expensive for large UAV-user networks. The authors in [19] proposed a distributed algorithm for joint 3D placement and user association in multi-UAV networks to optimize the network's sum rate. However, the algorithm has the shortcomings of not considering the energy efficiency and the users' traffic demands. In [2], a framework for joint user association and power control in cellular networks with a macro-base station (BS) and UAV aerial BS was proposed. The objective is to maximize network utility while considering power control, load balancing, and user fairness. However, the framework has some limitations, as it only maximizes the minimum signal-to-interference-plus-noise ratio (SINR) of all users without considering individual user demands. This results in not fully optimizing for the best user experience and demand satisfaction. In [20], a learning-based user association scheme for a dual UAV-enabled wireless network with device-to-device (D2D) connections in post-disaster scenarios was proposed. One shortcoming of this article is that it did not consider users' demands and users' power control. Additionally, the article assumed that only one user is connected to the UAV, and other users are waiting for that user to connect through D2D relaying, which could be a limitation. The authors in [21] proposed a load-balancing strategy for UAVs to support terrestrial networks by carrying BS toward areas with high traffic demands. The article introduced a clustering method to divide users into categories and initialize the positions of UAVs in the maximal local density areas. The main shortcoming of the proposed approach is that it only minimizes the maximum traffic demand of UAVs and neither considers the users' demands nor UE power control. Also, it attempted to solve the user association problem geographically by designing the service region of each UAV. The authors of [22] focused on a downlink cellular network where multiple UAVs serve as aerial BSs to provide wireless connectivity to ground users through a frequency division multi-access (FDMA) scheme by alternatively optimizing user association, resource allocation, and BS placement. However, the paper has two shortcomings. First, it did not consider the demand of users, which may result in some users being unserved or experiencing poor service. Second, it did not address power control, which can affect the energy efficiency of UEs and the overall network. The author of [23] discussed flying BSs mounted on UAVs as a substitute for conventional static BSs in dense deployment scenarios. The goal is to maximize user satisfaction with the provided data rates by proposing an algorithm that associates users with the most suitable static/flying BS and finds the optimal positions of all flying BSs. However, the paper did not consider the energy efficiency and users' demands.

To overcome the shortcomings of the UAV-user association and power control schemes existing in the literature, in this paper, the proposed bipartite graph-based UAV-user association maximizes the total achievable spectral efficiency of the multi-UAV-user network while considering users' demands and UAVs' capacities. Moreover, the M -matrix theory-based power control scheme optimizes the users' transmit power, maximizing their energy efficiency performance.

3. Proposed System Model

Figure 1 shows the proposed UAV-user network architecture, where multiple UAVs are deployed to provide communication services to users in remote and hard-to-reach areas.

The system model consists of two main components: the UAVs and the ground users. The UAVs are denoted by V and are located at a height of g , with the maximum number of M UAVs represented as $(v_1, v_2, v_3, \dots, v_M)$. The ground users are denoted by U and include a maximum number of N users, represented as $(u_1, u_2, u_3, \dots, u_N)$. The UAVs relay data and control signals to/from the distributed users. Moreover, UAVs have overlapping coverage, which means that some UE will be located under the coverage of multiple UAVs simultaneously. In this scenario, UAV-user association and UE power control are highly needed to maximize the overall network's spectral and energy efficiencies based on UAV-user link qualities, users' traffic demands, and UAVs' maximum capacities. This section will give the utilized UAV-UE channel model and the optimization problem formulation.

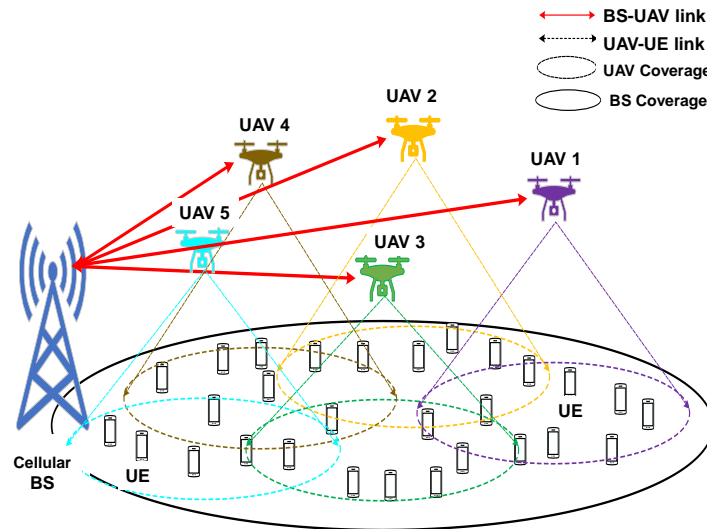


Figure 1. System model for deploying UAVs as communication base stations/relays in a post-disaster scenario, with varying numbers of UAVs and users.

3.1. UAV-UE Channel Model

The ground users u_i are represented by their locations $x_i^U = (x_1^U, x_2^U, \dots, x_N^U)$ in a two-dimensional space, where $x_i^U \in R^+$. Ground users' distribution is quasi-static, meaning their movements are negligible during the placement update process. As the considered use case is related to rescue services in post-disaster regions, it is reasonable to assume that UE mobility is quasi-static. This is because victims in post-disaster regions are less mobile due to the dangerous situations coming from damages after earthquakes or floods. Thus, UAVs will cover this region as long as both UAVs and UE have remaining battery capacities, and the UAVs' replacement will be conducted after their batteries are depleted and needed for recharging. In this scenario, the UAVs are hovering at a fixed altitude g and their locations are represented by $x_j^V = (x_1^V, x_2^V, \dots, x_M^V)$ projected onto the ground and $x_j^V \in R^+$. The ground distance between user i and UAV j is defined as r_{ij} , which is the distance between user i and the projections of UAV j on the ground, given by $r_{ij} = \|x_j^V - x_i^U\|$. The space distance between user i and UAV j is denoted by d_{ij} and is calculated as $d_{ij} = \sqrt{|r_{ij}|^2 + |g|^2}$.

In air-to-ground (A2G) standard communication systems, the quality of the wireless links between UAVs and ground users depends on the propagation environment. Two types of links can be distinguished: line-of-sight (LoS) and non-line-of-sight (NLoS) links. LoS links have a direct path between the transmitter (TX) and receiver (RX), while buildings, trees, or other objects obstruct NLoS links. Two different attenuation factors are typically utilized to account for the differences in signal attenuation between LoS and NLoS links. The path loss of the LoS and NLoS in the link L_{ij} between user i and UAV j is modeled as follows:

$$PL_{ij}^z = \left(\frac{4\pi f}{c}\right)^2 d_{ij}^2 \Sigma_{ij}^z, \quad z \in \{LoS, NLoS\} \tag{1}$$

where the values of the path losses PL_{ij}^{LoS} and PL_{ij}^{NLoS} depend on the carrier frequency f and the speed of light c . Typically, PL_{ij}^{LoS} is smaller than PL_{ij}^{NLoS} , as LoS links experience less attenuation than NLoS ones. The random variables Σ_{ij}^{LoS} and Σ_{ij}^{NLoS} represent the random fading of the wireless signal due to multipath propagation and other effects, which are estimated from empirical measurements or simulations. They are typically modeled as zero-mean Gaussian random variables with variances that depend on the environment and the frequency of the signals.

One common approach to evaluate the total path loss is to use the probabilistic LoS model, which does not explicitly depend on the dimensions of buildings and streets. In this model, the probability of the LoS path existence between a UAV and a ground user is determined by environment statistics and the elevation angle between UAV and ground user. Thus, the probability of a LoS link between user i and UAV j can be approximated using the following equation [24]:

$$\mathbb{P}_{ij}^{LoS} \approx \frac{1}{1 + a \exp(-b(\theta_{ij} - a))} \quad (2)$$

The constants a and b depend on the ratio of built-up land area to the total land area, the mean number of buildings per unit area, and the distribution of the buildings' heights [24]. The elevation angle from the ground user to the UAV, denoted by θ_{ij} , is given by [24]:

$$\theta_{ij} = 180 \arctan\left(\frac{g}{r_{ij}}\right), \quad (3)$$

The probability of NLoS link between user i and UAV j is $\mathbb{P}_{ij}^{NLoS} = 1 - \mathbb{P}_{ij}^{LoS}$. Thus, the total path loss between user i and UAV j can be written as follows:

$$PL_{ij} = \mathbb{P}_{ij}^{LoS} \times PL_{ij}^{LoS} + \mathbb{P}_{ij}^{NLoS} \times PL_{ij}^{NLoS}, \quad (4)$$

In this paper, uplink data transmission is assumed where uploaded data from victims and rescue workers are of the most significance for successful rescue operations. This includes real time locations of the victims, navigation assistance to reach save zones, communication with authorities, resource needs and priorities, identification and personal information of the victims, and their health stats updates, especially in the case of injuries. Moreover, reducing UE energy consumption is highly important due to the damaged electricity infrastructure. In this context, UE's TX powers are optimized based on the uplink data rates of the adjusted UAV-UE association pattern. Although uplink is considered in this paper, the proposed scheme can be applied for downlink as well, but using UAVs' TX powers instead of UE's. The received signal power Pr_{ij} at UAV j from user i is determined by the path loss and the fading channel, which is influenced by the distance between user i and UAV j , the TX power Pt_i of user i , and PL_{ij} , as follows [24]:

$$Pr_{ij} = \frac{Pt_i}{\left(\frac{4\pi f}{c}\right)^2 d_{ij}^2 \left(\mathbb{P}_{ij}^{LoS} \times \Sigma_{ij}^{LoS} + \mathbb{P}_{ij}^{NLoS} \times \Sigma_{ij}^{NLoS}\right)} \quad (5)$$

It is important to note that the UAV-UE channel model considered in this paper and given in (5) is a 2D channel model, i.e., assuming fixed UAV altitude, due to the following reasons: (1) UAVs are typically hovering at a fixed altitude during the communication period, which makes the assumption of UAVs' fixed height a practical one. (2) The proposed graph-based UAV-UE association and UE's TX power control mainly depend on the associated UAV-UE channels. Thus, considering 3D channel modeling by dynamically changing the UAVs' height will result in frequent UAV-UE association and UE's TX power control in accordance with UAVs' height changes. This makes the proposed approach unstable and highly time dependent. (3) In this paper, the UAVs' altitudes are considered high enough, e.g., 300 m, for enabling them to hover at fixed height and make the 2D channel model more realistic.

3.2. Optimization Problem Formulation

Based on Pr_{ij} given in (5), the SINR between user i and UAV j can be expressed as follows:

$$\psi_{ij} = \frac{Pr_{ij}}{\sum_{k \neq i}^{N_j} Pr_{kj} + \rho_{ij}}, \quad (6)$$

where ρ_{ij} is the noise power and $\sum_{k \neq i}^{N_j} Pr_{kj}$ is the sum of interference powers caused by the other users connected to UAV j , where N_j is the total number of users connected to UAV j . Thus, the data rate in link L_{ij} can be expressed as follows:

$$R_{ij} = B \log_2 (1 + \psi_{ij}), \quad (7)$$

where B is the utilized bandwidth. The data rate of the link L_{ij} in bit/sec, Ψ_{ij} , is defined as the minimum value between user traffic demand D_i in bit/sec and the achievable data rate R_{ij} , expressed as

$$\Psi_{ij} = \min (D_i, R_{ij}), \quad (8)$$

The performance metric Ψ_{ij} provides insights into how efficiently the system utilizes the available spectral resources, with higher values indicating more efficient utilization and lower values suggesting underutilization. In (5) to (7), we have considered the worst-case scenario, where all mutual UAV-UE links interfere with each other without using any centralized multiple access technique to distribute the available resources, i.e., frequency and time, among the mutual links. This will give the lower limit of system data rate performance while not increasing the complexity of the radio resource management.

Maximizing data rate is important in wireless communication system design to support higher data rates and accommodate more users, improving system performance. Thus, the optimization problem of UAV-user association and UE's TX power control can be formulated as follows:

$$\max_{I_{ij}, Pt_i} \sum_{j=1}^N \sum_{i=1}^M I_{ij} \Psi_{ij} \quad (9)$$

s.t

$$C1: I_{ij} \in \{0, 1\}$$

$$C2: \sum_{j=1}^M I_{ij} = 1, \forall i \in U$$

$$C3: \sum_{i=1}^N I_{ij} \geq 1, \forall j \in V$$

$$C4: \sum_{i=1}^N I_{ij} \Psi_{ij} \leq C_{jmax}, \forall j \in V$$

$$C5: Pt_i \in \{0, Pt_{max}\}, \forall i \in N$$

where I_{ij} is the binary association indicator, which is equal to 1 if user i is associated with UAV j and 0 otherwise. The 2nd constraint means that each user i should be associated with only one UAV, and the 3rd constraint means that many users can be associated with one UAV. The 4th constraint means that the sum of data rates to all users associated with UAV j should not exceed its maximum capacity C_{jmax} . Finally, the last constraint means that the TX power of UE i is non-negative and bounded by its maximum TX power Pt_{max} . This optimization problem is a mixed-integer linear programming (MILP) problem with binary and linear constraints. The objective is to find the optimal association indices and UE TX powers that maximize the sum of data rates in the system under the above constraints. It is well known in the literature that this kind of problem is an NP-hard one.

4. Proposed UAV-User Association and Power Control

This section will present the proposed approach for solving the optimization problem given in (9). The proposed approach is based on simplifying (9) by splitting it into two

sub-problems. In the first one, the UAV-user association matrix is optimized based on the achievable Ψ_{ij} while assuming all UE operates at its maximum TX power $P_{t_{max}}$. Then, the values of P_{t_i} 's are optimized based on the minimum UAV-user link qualities resulting from their tuned association matrix. The proposed algorithms are executed in a centralized manner, where a central controller or server located in the cellular BS shown in Figure 1 is responsible for optimizing the UAV-user association and UE TX power control. The central entity processes the information from the UAVs and UE, performs the necessary calculations based on the proposed algorithms, and then communicates the optimized association decisions and power control settings back to the UAVs and UE. This centralized approach allows for efficient coordination and optimization across the entire network.

4.1. Proposed Graph-Based UAV-User Association

In graph theory, a graph is a collection of nodes (vertices) and edges (lines) connecting them. Considering the connection between UAVs and UE, we can represent this as a bipartite graph with nodes representing the UAVs and UE while the edges represent the connections among them, as shown in Figure 2a. The graph is $G(U, V, L)$, where U represents the set of UE nodes and V represents the set of UAV nodes. An edge L_{ij} represents a connection between UE i and UAV j . In this context, the graph can be used to model the communication network between UAVs and UE, allowing for the analysis of factors such as network connectivity and capacity. In this paper, to find the best association indices I_{ij} maximizing the achievable total system capacity for the fixed $P_{t_i} = P_{t_{max}}$, we propose the MwMaxFlow approach based on the bipartite graph representation. The proposed approach consists of two algorithms: the MWM algorithm followed by the Maxflow algorithm. In the proposed MWM algorithm, UE is associated with UAVs maximizing their achievable Ψ_{ij} under the constraint that each UE should be connected to only one UAV as given in the 2nd constraint in (9) and as many UEs can be connected to one UAV as given in the 3rd constraint. On the other hand, the MaxFlow algorithm is proposed to maximize the achievable spectral efficiency of the whole UAV-UE network. This can be done by optimizing the flow of the UAV-UE links constructed by the MWM algorithm constrained by the maximum UAVs' capacities $C_{j_{max}}$ as given in the 4th constraint in (9).

4.1.1. Maximum Weighted Matching for UAV-UE Association

The proposed MWM algorithm is instrumental in our work, enabling us to optimize the UAV-UE association indices I_{ij} based on their corresponding Ψ_{ij} values. If a UE can be covered with more than one UAV, it will connect with the one maximizing its achievable Ψ_{ij} . For instance, consider the scenario depicted in Figure 2a. Let's take the example of UE₂, which can be associated with UAV₁ or UAV₂. If Ψ_{21} is higher than Ψ_{22} , then UE₂ will connect to UAV₁, and then I_{21} is set to 1 and I_{22} is set to 0. This process is applied to all users, determining their optimal UAV-UE associations as shown in Figure 2b.

4.1.2. MaxFlow for Spectral Efficiency Maximization

After applying the MWM algorithm to obtain the UAV-UE association matrix, the MaxFlow algorithm is used to maximize the flow of the whole network. In this regard, the Ford–Fulkerson MaxFlow algorithm is utilized; it is a widely used method for solving the maximum flow problem in graph theory. Compared with other algorithms, the Ford–Fulkerson algorithm does not prioritize finding the shortest path from the source node to the sink node. Instead, it focuses on augmenting paths that allow more flow until no more such paths exist, which is more appropriate to the considered UAV-user association problem. To apply the Ford–Fulkerson algorithm, we first add a source node S that is connected to each UE node i in graph G , and a sink node T that is connected to each UAV node j in the graph as shown in Figure 2c. This results in a new graph $G' = (U, V, L')$, where L' includes the links corresponding to $I_{ij} = 1$ between UE and UAV nodes obtained from the MWM algorithm as well as the added new links between the S node and UE nodes, and between the UAV nodes and T node. This creates a network where the flow can be directed from

the S node to the T node through the predefined associations between the UE and UAVs, as shown in Figure 2c.

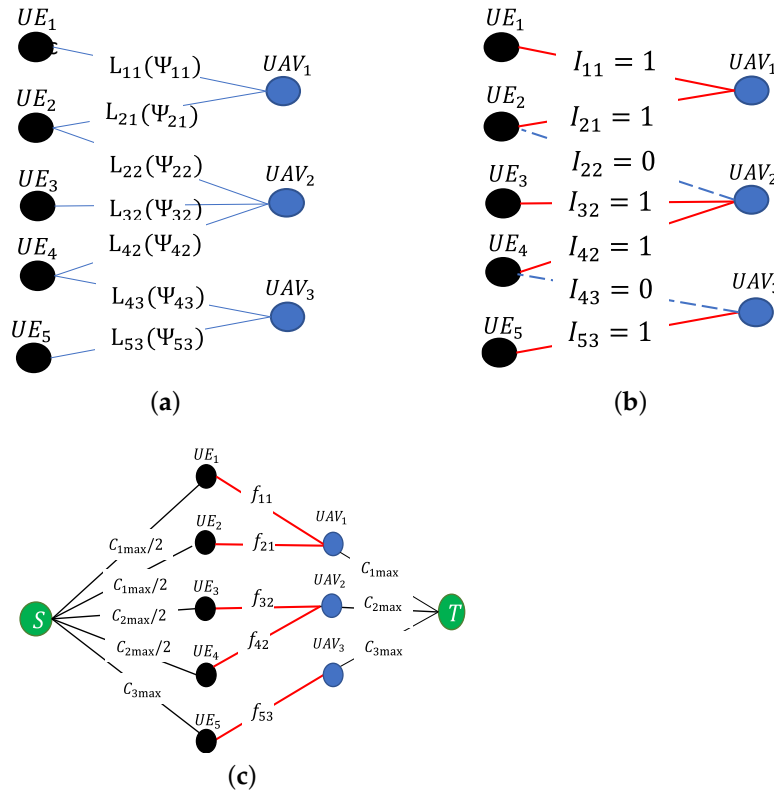


Figure 2. A bipartite graph where one set of nodes represents UE, and the other represents UAVs. The figure illustrates the application of the MWMMaxFlow approach to determine the maximum data flow from a source node S to a sink node T after associating them based on UE demands and the capacity constraints of the links; (a) The bipartite graph $G(U, V, L)$; (b) After applying the MWM Algorithm.; (c) After applying the MaxFlow algorithm on graph $G' = (U, V, L')$.

The objective of the MaxFlow algorithm is to maximize the total flow f between the UE and UAVs while considering the capacity constraints of the UAV nodes C_{jmax} as given in the 4th constraint in (9). This optimization problem can be formulated as follows:

$$\max \sum_{j=1}^M \sum_{i=1}^{N_j} f_{ij} \tag{10}$$

- s.t
- C1: $f_{ij} \in R^+, \forall i \in U, \forall j \in V$
 - C2: $f_{ij} \leq \Psi_{ij}, \forall i \in U, \forall j \in V$
 - C3: $f_{jT} \leq C_{jmax} \forall j \in V$
 - C4: $\sum_{i=1}^{N_j} f_{ij} - f_{jT} = 0, \forall j \in V$
 - C5: $\sum_{i=i}^N f_{Si} = \sum_{j=1}^M f_{jT}$

where f_{ij} represents the amount of data flow on the link L_{ij} , where $f = \sum_{j=1}^M \sum_{i=1}^{N_j} f_{ij}$. The 1st, 2nd, and 3rd constraints ensure that the flow in each link is positive and less than

or equal to its maximum capacity, i.e., Ψ_{ij} and C_{jmax} . The 4th constraint ensures flow continuity, i.e., the flow entering and leaving each UAV node is balanced. This constraint ensures that the UAVs properly receive all the data transmitted from the UE. The last constraint means that the flow leaving from S must equal that arriving at T . In Figure 2c, f_{si} are set to C_{jmax}/N_j to ensure fairness among the flows of the UE-to-UAV links and to ensure that all UE associated with UAV j will connect with it irrespective of the capacities required by the other augmented paths connected to UAV j .

In this paper, the Ford–Fulkerson algorithm is used to iteratively solve the optimization problem in (10) and maximize the total flow in the network. The algorithm iteratively searches for augmenting paths from S to T . In this context, an augmenting path has available capacity on all its edges. Finding an augmenting path entails traversing the network from S to T while considering only the edges with remaining capacity. If an augmenting path is discovered, the algorithm determines the maximum amount of flow that can be pushed through this path. This maximum flow is limited by the Ψ_{ij} of each link and the total UAV capacity C_{jmax} . The algorithm then adds this amount of flow to the flow values of the edges along the path. Then, the algorithm repeats the process of searching for augmenting paths and updates the flow until no more augmenting paths can be found. At this stage, the flow obtained represents the maximum flow that can be achieved in the network while adhering to the capacity constraints of the UAV nodes. It is worth noting that the proposed MWM algorithm allows the MaxFlow algorithm to maximize the total network flow based on the maximum Ψ_{ij} values, maximizing the overall spectral efficiency as challenged in (9). However, only applying the MaxFlow algorithm without the MWM algorithm will not maximize the overall spectral efficiency, as links with low Ψ_{ij} values may be selected to construct the UAV-UE links.

Algorithm 1 gives the proposed MwMaxFlow approach combining both the proposed MWM and the Ford–Fulkerson MaxFlow algorithms. The inputs are R_{ij} , D_i , $G(U, V, L)$, and C_{jmax} , and the outputs are the association binary indices I_{ij} and the maximum flow f_{max} . At first, the Ψ_{ij} values are calculated for $\forall i$ and $\forall j$ in graph G . Then, the MWM algorithm is applied to associate the UE to UAVs based on their maximum Ψ_{ij} value. After adjusting the I_{ij} values, the proposed Ford–Fulkerson MaxFlow algorithm is adopted to find f_{max} . At first, the graph $G' = (U, V, L')$ is constructed as shown in Figure 2c by considering the adjusted links corresponding to $I_{ij} = 1$ resulting from the MWM algorithm in addition to adding the S and T nodes. Also, the values of flows f_{ij} are initialized to 0, and the residual graph G'_r is initialized by G' . Then, all augmented paths from node S to node T are examined. For every augmented path p , its residual capacity, $\mu_r(p)$, is calculated as the minimum capacity of all edges included in this path, i.e., $\forall L'_{rij} \in p$. Then, this residual capacity is added to the total flow of the network. Furthermore, all edges of this path are tested to see if they are forward or backward edges. If an edge in the path p is identified as forward, its capacity μ_{rij} is decreased by the value of $\mu_r(p)$; otherwise, it is increased by the value of $\mu_r(p)$, as it has been identified as a backward path. After adjusting the new capacities, the residual graph G'_r is updated for the next selection of another augmented path. This process is repeated till the final augmented path in the network has been identified. Finally, the value of f_{max} is set to equal the obtained value of f .

4.2. Power Control

One of the efficient ways to improve energy efficiency in wireless communication systems is to reduce the TX power of the involved devices to be lower than their maximum values. This can be achieved by optimizing them based on the required minimum link quality. This approach not only reduces energy consumption but also has the advantage of reducing interference among devices. However, lowering the transmission power may decrease the signal quality, which can be caused by interference from other devices in the network. Therefore, it is essential to design an effective power control mechanism that can conserve energy, reuse bandwidth more efficiently, and maintain the quality of communication at an acceptable level.

Algorithm 1: Proposed MwMaxFlow Approach

```

Output:  $I_{ij}, f_{max}$ 
Input:  $R_{ij}, D_i, G(U, V, L), C_{jmax}$ 
Initialization: Calculate  $\Psi_{ij} = \min(R_{ij}, D_i)$  for  $\forall i$  and  $\forall j$ .
  • The MWM Algorithm to Optimize  $I_{ij}$ 

for  $i = 1, 2, \dots, N$  do
  | for  $j = 1, 2, \dots, M$  do
  | | if  $\Psi_{ij} \neq 0$  then
  | | |  $i = \arg \max_j \Psi_{ij}$ 
  | | |  $I_{ij} = 1$ 
  | | else
  | | |  $I_{ij} = 0$ 
  | | end
  | end
end

  • The Ford-Fulkerson MaxFlow Algorithm to Optimize  $f_{max}$ 

Input: Construct  $G' = (U, V, L')$  consisting of the links corresponding to
 $I_{ij} = 1$  between UE and UAV nodes obtained from the MWM Algorithm in
addition to adding  $S$  and  $T$  nodes as shown in Figure 2c.

Initialization:  $f_{ij} = 0 \forall L' \in G', G'_r = G'$ 
1 while There is an augmented path  $p$  in  $G'_r$  do
  |  $\mu_r(p) = \min_{\forall L'_{rij} \in p} (\mu_{rij})$ 
  |  $f = f + \mu_r(p)$ 
  | for  $\forall L'_{rij} \in p$  do
  | | if  $L'_{rij}$  is a forward edge then
  | | |  $\mu_{rij} = \mu_{rij} - \mu_r(p)$ 
  | | else
  | | |  $\mu_{rij} = \mu_{rij} + \mu_r(p)$ 
  | | end
  | end
  | Update the residual network  $G'_r$ 
end
 $f_{max} = f$ 

```

The proposed approach in this study employs the M -matrix theory to optimize the TX power of the UE and improve energy efficiency, as considered in [30,31]. It is assumed that the minimum link quality of an edge between UE and UAV is equal to its adjusted flow f_{ij} resulting from the MaxFlow algorithm, which corresponds to a minimum SINR quality of $(\psi_{f_{ij}} = 2^{(f_{ij}/B)} - 1)$ based on (7). Thus, the optimization problem for maximizing energy efficiency while ensuring the quality of communication can be formulated as follows [30,31].

$$\min_{P_{t_i}} \sum_i^N P_{t_i}$$

s.t

$$C1 : \psi_{ij} = \psi_{f_{ij}}, \forall i \in N \text{ and } \forall j \in M \quad (11a)$$

$$C2 : P_{t_i} \in \{0, P_{t_{max}}\}, \forall i \in N \quad (11b)$$

This problem is a kind of convex optimization problem. For a single UAV j with N_j associated UE, this problem can be formulated as the solution to the set of linear equations as follows:

$$\frac{P_{t_i} |h_{ij}|^2}{\psi_{f_{ij}}} - \sum_{k=1, k \neq i}^{N_j} P_{t_k} |h_{kj}|^2 = \rho_{ij}, \quad (12)$$

where $|h_{ij}|^2$ is the channel gain between UE i and UAV j , while $|h_{kj}|^2$ is the channel gain between UE k , $k \neq i$ and UAV j . These channels are calculated based on the path loss model given in Section 3.1. Using matrix-vector notation, (12) can be expressed as follows:

$$\mathbf{A}_j \mathbf{P}_{tj} = \mathbf{w} \Rightarrow \mathbf{P}_{tj} = \mathbf{A}_j^{-1} \mathbf{w}, \tag{13}$$

where

$$\mathbf{A}_j = \begin{pmatrix} |h_{1j}|^2/\psi_{f_{1j}} & -|h_{2j}|^2 & -|h_{3j}|^2 & \dots & -|h_{N_jj}|^2 \\ -|h_{1j}|^2 & |h_{2j}|^2/\psi_{f_{2j}} & -|h_{3j}|^2 & \dots & -|h_{N_jj}|^2 \\ -|h_{1j}|^2 & -|h_{2j}|^2 & |h_{3j}|^2/\psi_{f_{3j}} & \dots & -|h_{N_jj}|^2 \\ -|h_{1j}|^2 & -|h_{2j}|^2 & -|h_{3j}|^2 & \ddots & -|h_{N_jj}|^2 \\ \vdots & \vdots & \vdots & \vdots & \vdots \\ -|h_{1j}|^2 & -|h_{2j}|^2 & -|h_{3j}|^2 & \dots & |h_{N_jj}|^2/\psi_{f_{N_jj}} \end{pmatrix} \tag{14}$$

$$\mathbf{P}_{tj} = \begin{pmatrix} Pt_{1j} \\ Pt_{2j} \\ Pt_{3j} \\ \vdots \\ Pt_{N_jj} \end{pmatrix} \text{ and } \mathbf{w} = \rho_{ij} \begin{pmatrix} 1 \\ 1 \\ 1 \\ \vdots \\ 1 \end{pmatrix} \tag{15}$$

$$\mathbf{Q}_j = \text{diag} \left(h_{ij} \left[1 + \frac{1}{\psi_{f_{ij}}} \right] \right), \mathbf{1}_{N_j} = \begin{pmatrix} 1 \\ 1 \\ 1 \\ \vdots \\ 1 \end{pmatrix} \text{ and } \Delta_j^T = \begin{pmatrix} h_{1j} \\ h_{2j} \\ h_{3j} \\ \vdots \\ h_{N_jj} \end{pmatrix}^T \tag{16}$$

It should be noted that \mathbf{A}_j of size $N_j \times N_j$ is a \mathcal{Z} -matrix as described in [31], i.e., it is a matrix whose off-diagonal elements are non-positive. To solve for \mathbf{P}_{tj} as represented in (13), \mathbf{A}_j should be an \mathcal{M} -matrix as well, where a \mathcal{Z} -matrix is called an \mathcal{M} -matrix if its inverse has all non-negative elements. To solve (13) by obtaining \mathbf{A}_j^{-1} , we will utilize the Sherman–Morrison formula [32]. To do so, \mathbf{A}_j is rewritten as follows:

$$\mathbf{A}_j = \mathbf{Q}_j - \mathbf{1}_{N_j} \Delta_j^T \tag{17}$$

In the Sherman–Morrison theorem [32], the inverse of any off-diagonal singular square matrix, in the form of (17), can be calculated as follows:

$$\mathbf{A}_j^{-1} = \mathbf{Q}_j^{-1} + \frac{\mathbf{Q}_j^{-1} \mathbf{1}_{N_j} \Delta_j^T \mathbf{Q}_j^{-1}}{1 - \Delta_j^T \mathbf{Q}_j^{-1} \mathbf{1}_{N_j}}, \tag{18}$$

However, there is a necessary condition for finding a feasible non-negative solution for \mathbf{P}_{tj} using (18), which is:

$$\sum_{i=1}^{N_j} \left(1 + \frac{1}{\psi_{f_{ij}}} \right)^{-1} < 1 \tag{19}$$

The proof of this condition comes straightforwardly from (17), where \mathbf{Q}_j , $\mathbf{1}_{N_j}$, and Δ_j^T are all positive diagonal matrices and vectors as shown in (18). Thus, from (19), \mathbf{A}_j is an \mathcal{M} -matrix, i.e., \mathbf{A}_j^{-1} has all non-negative elements if and only if the denominator $(1 - \Delta_j^T \mathbf{Q}_j^{-1} \mathbf{1}_{N_j} > 0)$, i.e., $\Delta_j^T \mathbf{Q}_j^{-1} \mathbf{1}_{N_j} < 1$, which yields to (19) using (18). However, the condition in (19) only guarantees the lower bound condition of \mathbf{P}_{tj} , i.e., $\mathbf{P}_{tj} \geq 0$ without the upper bound one, i.e., $\mathbf{P}_{tj} \leq Pt_{max}$. Thus, the solution of \mathbf{P}_{tj} obtained via (18) should be limited by its maximum value of Pt_{max} .

5. Numerical Analysis

In this section, we present a detailed overview of the simulation setup to provide a comprehensive understanding of the simulation conditions. The Monte Carlo numerical simulations were conducted in a carefully chosen area spanning 2500 m², representing a realistic scenario for UAV-assisted wireless communication networks. The network configuration involved the deployment of up to 10 UAVs strategically positioned at an altitude of 300 m, with both UAVs and UE uniformly distributed across the simulation area to capture diverse spatial arrangements. The carrier frequency for UAV-UE links was set at 2 GHz, aligning with common sub-6GHz wireless communication standards, and a total bandwidth of 20 MHz was allocated. To accurately model the UAV-UE channel, path loss parameters were considered, with path loss in LoS and NLoS conditions characterized by 0.1 and 21 dB, respectively. These parameters played a pivotal role in determining the signal quality and link characteristics. Transmission power constraints were defined to regulate communication, with a maximum UE transmission power of 24 dBm. The maximum capacity for each UAV was determined by the available bandwidth and maximum transmission power, following the formula $C_{jmax} = B \log_2(1 + P_{tmax}/\rho_{ij})$, where ρ_{ij} (dBm) = $-174 + 10 \log_{10}(B) + 10$. These critical simulation parameters are listed in Table 1, unless otherwise stated.

Table 1. Simulation parameters.

Parameter	Value
f, B	2 GHz [19], 20 MHz [18]
g	300 m
$\Sigma_{ij}^{LoS}, \Sigma_{ij}^{NLoS}$	0.1 dB and 21 dB [18]
f_V, f_S	2 GHz [18], 2.4 GHz [19]
ρ_{ij} (dBm)	$-174 + 10 \log_{10}(B) + 10$ [7]
a, b	4.88, 0.429 [18]
P_{tmax}	24 dBm [18]
C_{jmax}	$B \log_2(1 + P_{tmax}/\rho_0)$

For performance comparisons, we compared the proposed approach with basic comparable schemes, as there is no scheme existing in the literature addressing the same problem. The legend in the simulation figures represents different methods involved in the comparisons. The random selection method “RS” randomly selects associations between users and UAVs without any specific target. “MRP” refers to the maximum received power method, which selects associations to maximize the received power at UAVs. The “MaxFlow” algorithm only uses the maximum flow algorithm. Finally, “MwMaxFlow” indicates the proposed approach. These methods provide different approaches to optimize UAV-user associations, and, as we previously explained, we selected them as no comparable scheme was proposed in the literature for addressing the same problem.

5.1. Performance Comparisons without Using Power Control

Figure 3 shows the data rate in bit/sec against the number of sets of UE using 10 UAVs, where the UE is operating at its maximum TX power of P_{tmax} . If the number of sets of UE is set to 10, almost all schemes involved in the comparisons have the same data rate performance because the network is lightly dense and only a few sets of UE are under the overlapping coverage of UAVs, and in some cases, each UAV has only one UE associated with it. However, if the number of sets of UE is tremendously increased, the network becomes heavily dense and many sets of UE will be under the overlapping coverage of multiple UAVs. Thanks to their capabilities of maximizing the network flow, both the proposed “MwMaxFlow” and the “MaxFlow” schemes demonstrate higher data rate performances

than the “MRP” and “RS” schemes. If the number of sets of UE is set to 100, the proposed “MwMaxFlow” algorithm yields the highest data rate of 0.47 Gbps, which is 96% higher than that obtained by the ordinary “MaxFlow” algorithm, which has a data rate of 0.24 Gbps. This comes from the high capability of the proposed scheme in optimizing UAV-user association as well as maximizing the network flow. The “RS” approach achieves a data rate of 0.125 Gbps, representing a 3.76-time decrease from the proposed “MwMaxFlow” algorithm. On the other hand, the “MRP” algorithm achieves better performance than the “RS” scheme with a data rate of 0.15 Gbps, which is a 3.13-time decrease from the proposed “MwMaxFlow” algorithm. For energy efficiency (EE) in bit/joule without power control, the results from the conducted numerical simulations are shown in Figure 4, where the EE is evaluated as follows:

$$EE = \frac{\sum_{j=1}^M \sum_{i=1}^{N_j} I_{ij} \Psi_{ij}}{\sum_{i=1}^N Pt_i} \tag{20}$$

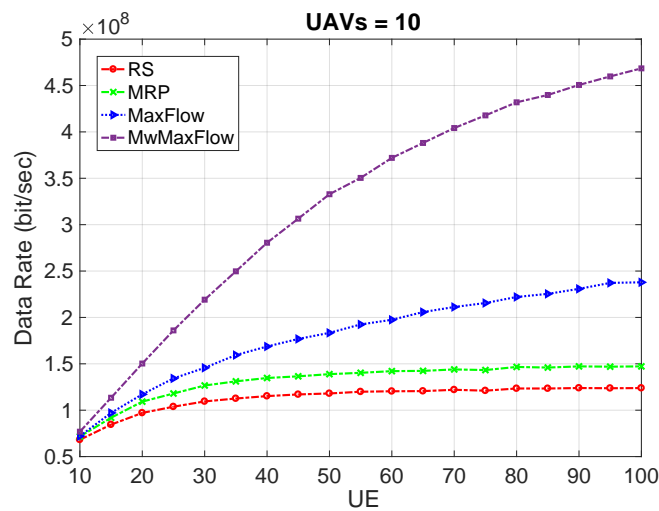


Figure 3. Data rate against the number of sets of UE using 10 UAVs without UE power control.

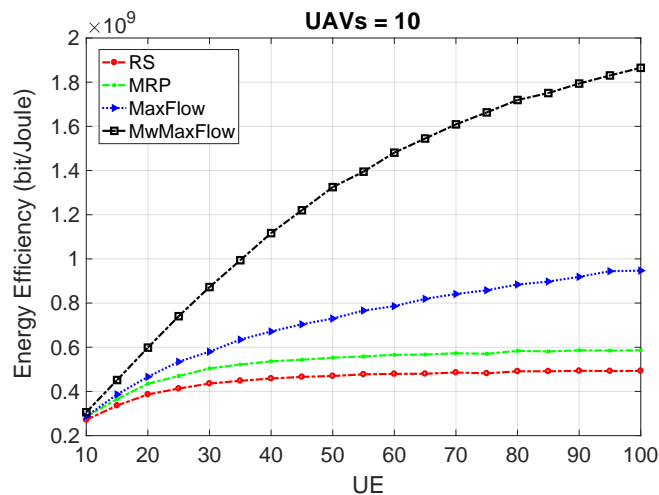


Figure 4. Energy efficiency against the number of sets of UE using 10 UAVs without UE power control.

In this figure, energy efficiency is evaluated against the number of sets of UE using 10 UAVs while all UE uses its maximum TX power, i.e., $Pt_i = Pt_{max}$. Compared with Figure 3, the energy efficiencies of all compared schemes have the same trend presented in Figure 3 but with different Y-axis values due to the use of fixed power allocation in the denominator of (20). As clearly shown, the proposed “MwMaxFlow” has the best energy efficiency performance, especially in dense networks with many users. Influenced by the

data rate performance presented in Figure 3, when the number of sets of UE is equal to 10, almost equal energy efficiency performance of the schemes involved in the comparison is obtained. As previously explained, this comes from the lightly dense network where few UEs will be under the overlapping coverage of some UAVs. However, as the network becomes dense, many users will be under the overlapping coverage of many UAVs, resulting in the superior energy efficiency performance of the proposed scheme. This comes from its superiority in optimizing the network and maximizing its traffic flow based on users' demands and UAVs' capacities. From Figure 4 and when the number of sets of UE is equal to 100, the results demonstrate that the proposed "MwMaxFlow" algorithm achieves the highest energy efficiency with a remarkable value of 1.85 Gb/Joule. The "MaxFlow" algorithm performs at a lower level of 0.98 Gb/Joule, while the "RS" algorithm yields a further reduction to 0.5 Gb/Joule. However, the "MRP" algorithm shows a moderate improvement of 0.6 Gb/Joule. These findings highlight the substantial differences in energy efficiency performance among the compared schemes.

Figure 5 presents the data rate as a function of the number of UAVs when 100 sets of UE are deployed without the use of power control. For scenarios where only two UAVs cover the area, both the "RS" and "MRP" schemes demonstrate similar data rates due to the limited spatial coverage. With a few UAVs, the chances of the UE experiencing overlapping coverage with many UAVs is diminished, resulting in a comparable data rate. Moreover, when there are only two UAVs, the proposed "MwMaxFlow" and "MaxFlow" schemes exhibit similar data rates due to the constrained UAVs' spatial coverage and relatively small number of UAVs. However, as the number of UAVs increases while maintaining 100 sets of UE, the data rate improves notably. This improvement can be attributed to the enhanced spatial coverage and better allocation of UE among multiple UAVs, which reduces mutual interference. Consequently, the data rate increases as UE is assigned to UAVs with better channel conditions. Again, as the proposed "MwMaxFlow" optimizes the UAV-user association based on the maximum achievable data rate, it demonstrates the best performance. In Figure 5, with two UAVs, the "RS" and "MRP" schemes achieve approximately 800 Mbps, while the "MaxFlow" and "MwMaxFlow" algorithms achieve significantly higher data rates at around 0.12 Gbps. On the other hand, with 10 UAVs covering the area, the data rate varies among the algorithms, with "RS" achieving approximately 0.12 Gbps, "MRP" achieving around 0.15 Gbps, "MaxFlow" performing better at 0.24 Gbps, and the proposed "MwMaxFlow" algorithm surpassing all others with the highest data rate of 0.46 Gbps. By comparing Figures 3 and 5, it is noted that the data rate of the case of 2 UAVs and 100 sets of UE is better than the case of 10 UAVs and 10 sets of UE for all schemes involved in the comparisons. This comes from having 10 times the number of sets of UE with higher data rates and traffic demands.

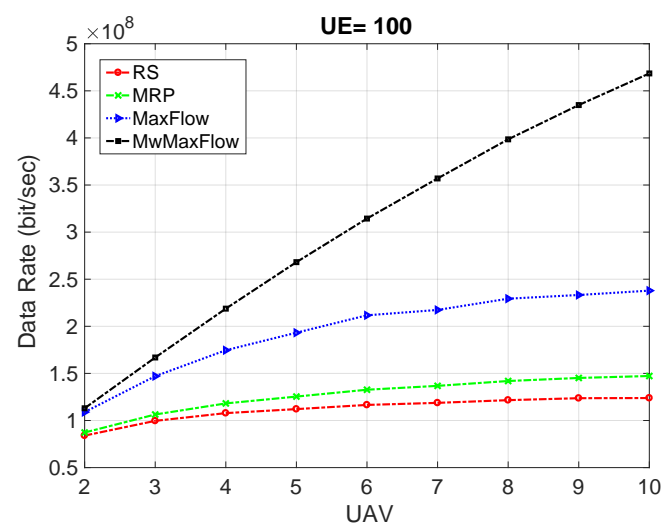


Figure 5. Data rate against the number of UAVs using 100 sets of UE without UE power control.

Figure 6 demonstrates the evaluation of energy efficiency for a fixed number of 100 sets of UE while varying the number of UAVs, which is influenced by the data rate performance given in Figure 5. Due to the use of fixed power allocation, Figures 5 and 6 have similar trends to Figures 3 and 4, but with different Y-axis values. When there are only 2 UAVs covering the area of 100 sets of UE, both the “RS” and “MRP” schemes exhibit a similar energy efficiency of 0.35 Gbit/Joule due to the aforementioned reasoning. On the other hand, the proposed “MwMaxFlow” and the “MaxFlow” schemes demonstrate higher energy efficiency than both “RS” and “MRP” schemes of 0.42 Gbit/Joule. As the number of UAVs increases, the energy efficiency of all algorithms improves, with “MwMaxFlow” achieving the highest energy efficiency at approximately 1.85 Gbit/Joule, followed by “MaxFlow” at 0.95 Gbit/Joule, “MRP” at 0.6 Gbit/Joule, and RS at 0.5 Gbit/Joule.

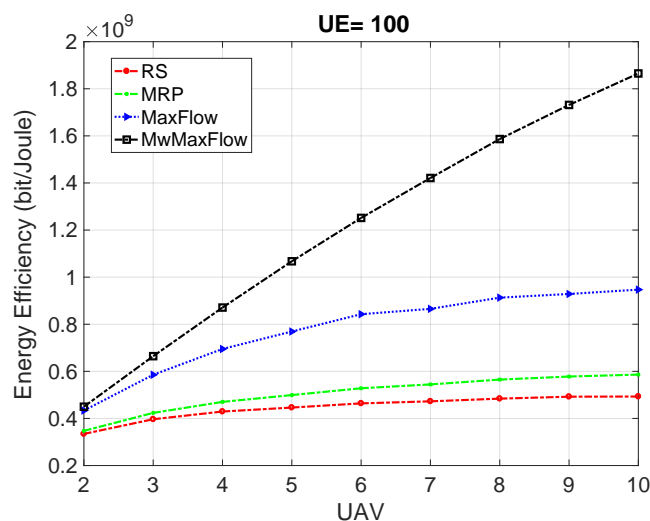


Figure 6. Energy efficiency against the number of UAVs using 100 sets of UE without UE power control.

5.2. Performance Comparisons with Using Power Control

Figures 7 and 8 give the results of the data rate performances of the proposed MwMaxFlow and the ordinary MaxFlow algorithms when considering a fixed number of sets of UE (UAVs) while increasing the number of UAVs (sets of UE), respectively. This is done for both the cases of including and not including power control (PC). It is clearly shown by these figures that the data rates of both algorithms with PC surpass their counterparts without PC. The theoretical underpinnings of the presented results lie in the minimization of UE TX power by utilizing the M -matrix theory. The subsequent application of these optimized power levels results in a notable enhancement in data rates due the reduced interference levels among the mutual UAV-UE links as presented in Figures 7 and 8. In other words, power control is employed to minimize UE TX power while upholding the minimum link qualities derived from maximizing the total network flow. This strategic interplay between maximizing the network flow and minimizing UE TX power unfolds as a key factor in achieving an optimal balance between maximizing spectral efficiency and minimizing energy consumption. In the proposed MwMaxFlow with PC, the sophisticated combination of graph theory-based UAV-UE association and M -matrix theory-based power control maximizes the overall network performance over the ordinary MaxFlow algorithm, which only maximizes the network flow without optimally associating UE to UAVs.

When using a fixed number of 100 sets of UE while increasing the number of UAVs till reaching 10 UAVs as presented in Figure 7, the data rate reaches 0.53 Gbits/sec for MwMaxFlow with PC compared with 0.48 Gbits/sec for MwMaxFlow without PC. When comparing with the MaxFlow approach, MwMaxFlow with PC demonstrates superior performance, which is 1.4 times higher than that of MaxFlow with PC. When using a constant number of 10 UAVs while increasing the number of sets of UE as presented in Figure 8, the influence of increasing UE on data rates becomes apparent. Specifically, when using 100 sets

of UE, the data rate of MwMaxFlow with PC is higher than that without PC by 1.11 times, and this value becomes 1.58 times in the case of using the ordinary MaxFlow algorithm. From the results presented in both figures, it is interesting to note that the data rate improvements when using PC with the ordinary MaxFlow are higher than that when using it with the proposed MwMaxFlow algorithm. This is because, in the proposed MwMaxFlow, the first stage of optimal UAV-UE association conducted by the proposed MWM algorithm highly reduces the mutual interference among the constructed UAV-UE links. Thus, power control will slightly further reduce this interference, and then slightly increase the achievable data rate. However, in the case of the ordinary MaxFlow, this UAV-UE association functionality does not exist, so it suffers from high mutual interference, which is substantially reduced by using power control, resulting in high improvements in the achievable data rate. This observation underscores the pivotal role of power control in optimizing data rates and, consequently, the overall performance of UAV networks under these scenarios.

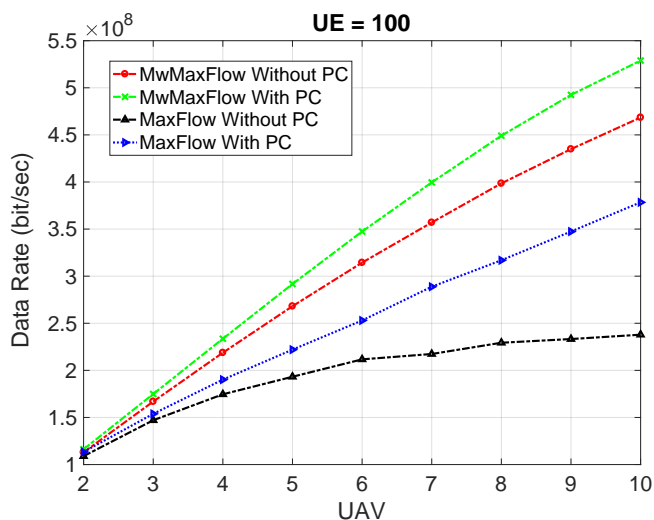


Figure 7. Data rate with and without using UE power control for the proposed “MwMaxFlow” and “MaxFlow” algorithms against the number of UAVs while using a fixed number of 100 sets of UE.

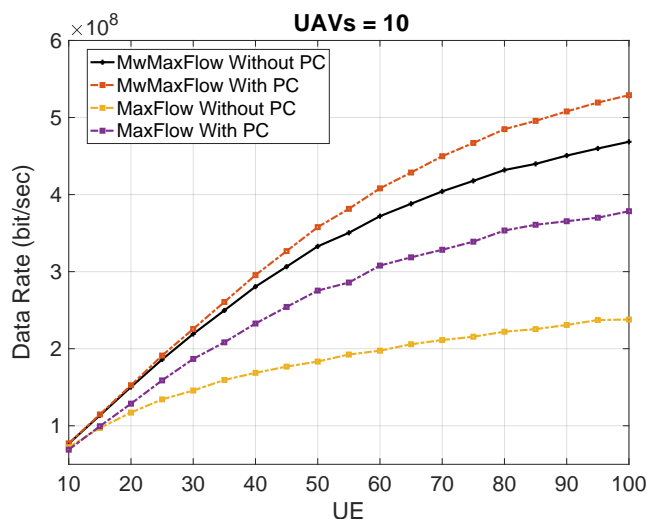


Figure 8. Data rate with and without using power control for the proposed “MwMaxFlow” and “MaxFlow” algorithms against the number of sets of UE while using a fixed number of 10 UAVs.

Figures 9 and 10 study the effect of PC on the energy efficiency performance of the proposed “MwMaxFlow” and the ordinary “MaxFlow” algorithms under different scenarios. Figure 9 presents the energy efficiency in bit/Joule on a logarithmic scale, demonstrating

power control schemes' impact on energy efficiency against the number of UAVs while using a fixed number of 100 sets of UE. Generally, as the number of UAVs increases, the energy efficiency performance improves. This is because with more UAVs deployed, there are better options for UE selection. This reduces the mutual interference, allowing for lower UE TX power levels while maintaining satisfactory signal quality. In contrast, limited UAVs may lead to higher mutual interference, higher UE TX power levels, and lower energy efficiency. Without using UE TX power control, the energy efficiency performance of the proposed "MwMaxFlow" and "MaxFlow" algorithms is relatively low. However, when power control is applied, significant improvements are observed. When there are only two UAVs covering the 100 UEs, both algorithms show similar energy efficiency levels with and without using power control due to the high-power interference due to the large number of sets of UE competing for the resources of only two UAVs. This reduces energy efficiency as more power is spent to overcome interference. However, when increasing the number of UAVs to 10 UAVs, the proposed "MwMaxFlow" algorithm outperforms the "MaxFlow" algorithm in both the cases of using and not using power control. In the case of not using power control, the proposed "MwMaxFlow" has higher energy efficiency performance than "MaxFlow" by almost two times, while the improvement reaches 2.3 when using power control. This is because the proposed "MwMaxFlow" algorithm handles UAV-user association based on the best channel conditions using the MWM algorithm, while the "MaxFlow" algorithm handles it irrespective of their channel conditions. Thus, in low interfering scenarios when using 10 UAVs, the A_j^{-1} matrix of the proposed algorithm has lower values than those belonging to the "MaxFlow" algorithm, which reduces its UE TX power consumption in consequence.

Figure 10 gives the energy efficiency performance of the "MwMaxFlow" and "MaxFlow" algorithms in the scenario of using 10 UAVs while varying the number of sets of UE. Like Figure 9, this figure clearly demonstrates that the application of power control significantly improves the energy efficiency of both schemes. Using 10 sets of UE, both schemes have the same energy efficiency performance without using power control, influenced by their similar data rate performances given in Figures 3 and 8. However, when using power control, the proposed "MwMaxFlow" achieves higher energy efficiency than "MaxFlow" by 1.8 times. When increasing the number of sets of UE to 100, the proposed "MwMaxFlow" outperforms "MaxFlow" by 2 times without using power control and 2.3 when using power control. This comes from assigning UE to UAVs with better channel conditions via the proposed scheme, which results in reducing their required TX power while maintaining satisfactory signal quality.

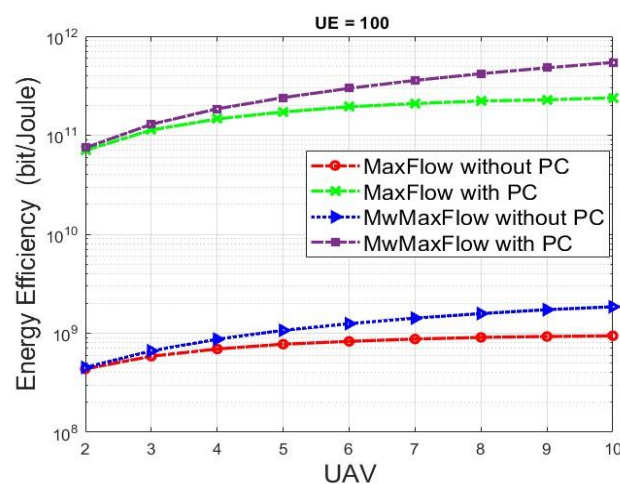


Figure 9. Energy efficiency with and without using UE power control for the proposed "MwMaxFlow" and "MaxFlow" algorithms against the number of UAVs while using a fixed number of 100 sets of UE.

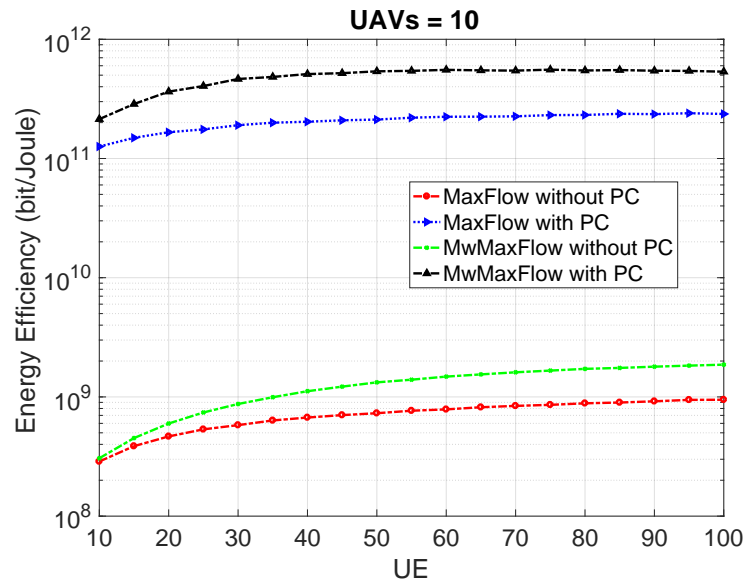


Figure 10. Energy efficiency with and without using power control for the proposed “MwMaxFlow” and “MaxFlow” algorithms against the number of sets of UE while using a fixed number of 10 UAVs.

It is worth comparing the results presented in Figures 9 and 10 for the cases of 2 UAVs and 100 sets of UE presented in Figure 9 and the case of 10 UAVs and 10 sets of UE presented in Figure 10. When not using power control, the energy efficiency presented in Figure 9 is higher than that given in Figure 10, but the opposite happens when using power control for the compared two cases. This comes from the higher spectral efficiency of the first case compared with the second one, as shown in Figures 3 and 5, owing to the having 10 times as many sets of UE in the first case. However, when using power control, this considerable amount of UE causes very high mutual interference compared with the second case, making the UE operate at higher TX powers than in the second case to withstand this high mutual interference. This results in the higher energy efficiency performance of the second case over the first one, as presented in Figures 9 and 10.

5.3. Complexity Analysis

For the computational complexity analysis, the computational complexity of the proposed approach consists of two parts; one is related to the MwMaxFlow algorithm, i.e., Algorithm 1, and the other is related to the power control scheme. For Algorithm 1, its computational complexity comes from three portions: (1) the calculations of $\Psi_{ij}, \forall i, j$ with a computational complexity of $O(NM)$, (2) the MWM algorithm to optimize I_{ij} with a computational complexity of $O(NM)$, and (3) the Ford–Fulkerson MaxFlow algorithm to optimize f_{max} with a computational complexity of $O(UV)$. Thus, the total computational complexity of Algorithm 1 will be $O(2NM) + O(UV)$. For the proposed M -matrix theory-based power control scheme, its computational complexity comes from (13), which consists of matrix inversion \mathbf{A}_j^{-1} with a computational complexity of $O(N_j^3)$ using standard matrix inversion, and a matrix-vector multiplication $\mathbf{A}_j^{-1}\mathbf{w}$ with a computational complexity of $O(N_j^2)$. Thus, the upper limit of the computational complexity of the UE TX power control becomes $O(N^3) + O(N^2)$, when $N_j = N$. Thus, the upper total computational complexity of the proposed approach including both the MwMaxFlow algorithm and TX power control will be $O(2NM) + O(UV) + O(N^3) + O(N^2)$.

6. Limitations of The Proposed Approach

While the proposed approach makes notable strides in optimizing UAV-user association and UE’s TX power control, it is imperative to acknowledge its inherent limitations. Firstly, although the assumption of uniformly UAV and UE distribution simplifies the analysis, it may not fully capture the intricacies of real-world deployments. Thus, more

realistic UAV and UE distributions coming from real field measurement campaigns should be considered in future investigations. Secondly, although the fixed UAVs' altitude could be a realistic assumption as UAVs hover at fixed altitudes, enabling us to consider 2D UAV-UE channel modeling, it could represent a limitation in highly dynamic environments. In this scenario, each UAV hovers at a different altitude, presenting a 3D UAV-UE channel model. These dynamic altitude adjustments based on network demands and environmental factors should be a subject of further exploration by proposing dynamic UAV-UE associations and UE power control schemes. Finally, in the current study, we only considered UE power control due to its importance, especially in post-disaster scenarios. However, in the situations when UAV battery recharging or its limited battery budget present critical factors in its mission span, optimizing UAVs' power through efficient power control mechanisms becomes a necessity and is valuable to be considered for future investigations.

7. Conclusions

This paper addressed the problem of optimal UAV-user association and UE TX power control in multiple UAV-user networks. The problem was formulated as an optimization problem under its essential constraints. Then, a bipartite graph-based UAV-user association was proposed to address the problem, namely "MwMaxFlow", which consists of two algorithms. The first algorithm handled the UAV-user association problem by linking users to UAVs, maximizing their achievable data rates while considering users' traffic demands. The second algorithm maximized the total network flow based on the UAV-user association conducted in the first step while considering the maximum UAV capacities. After maximizing the flow in each link, UE TX power control utilizing the M -matrix theory was applied to minimize UE TX power while maintaining the minimum link quality optimized by the network flow. Numerical simulations were performed to evaluate the proposed approach and compare its performance with other benchmark schemes. The results indicate that the proposed approach balances spectral efficiency and energy consumption, making it suitable for various UAV wireless applications, including emergency response, surveillance, and post-disaster management.

Although this study is a stepping stone toward addressing the multifaceted challenges in UAV communication networks, several avenues for future investigations emerge. Firstly, the exploration of dynamic and adaptive UAV altitude adjustments, responsive to network conditions and environmental factors, could enhance the efficiency and adaptability of the proposed approach. Secondly, the integration of realistic UAV energy consumption models is essential to comprehensively evaluate the sustainability of the network. Furthermore, the extension of the proposed methodology to consider varying UAV sizes and incorporate real-world data could provide a more accurate reflection of operational scenarios. Lastly, the potential integration of machine learning and artificial intelligence techniques for intelligent decision-making in UAV-user association warrants exploration. In essence, this study lays the groundwork for future investigations, aiming to refine and extend the proposed approach for the evolving challenges and opportunities in UAV communication networks.

Author Contributions: Conceptualization, M.A. and E.M.M.; Formal analysis, M.A. and E.M.M.; Investigation, M.A. and E.M.M.; Methodology, M.A. and E.M.M.; Resources, M.A. and E.M.M.; Software, M.A. and E.M.M.; Validation, M.A., E.M.M., W.M.A., and S.H.; Visualization, M.A.; Writing—original draft, M.A. and E.M.M.; Writing—review & editing, E.M.M., W.M.A., and S.H. All authors have read and agreed to the published version of the manuscript.

Funding: The authors extend their appreciation to Prince Sattam bin Abdulaziz University for funding this research work through the project number (PSAU/2023/01/DEC 2023-25).

Data Availability Statement: Data are contained within the article.

Conflicts of Interest: The authors declare no conflicts of interest.

References

1. Mozaffari, M.; Saad, W.; Bennis, M.; Nam, Y.H.; Debbah, M. A Tutorial on UAVs for Wireless Networks: Applications, Challenges, and Open Problems. *IEEE Commun. Surv. Tutor.* **2019**, *21*, 2334–2360.
2. Hashesh, A.O.; Hashima, S.; Zaki, R.M.; Fouda, M.M.; Hatano, K.; Eldien, A.S.T. AI-Enabled UAV Communications: Challenges and Future Directions. *IEEE Access* **2022**, *10*, 92048–92066.
3. Alnakhli, M. Optimizing spectrum efficiency in 6G multi-UAV networks through source correlation exploitation. *EURASIP J. Wirel. Commun. Netw.* **2024**, *2024*, 6.
4. Fotouhi, A.; Qiang, H.; Ding, M.; Hassan, M.; Giordano, L.G.; Garcia-Rodriguez, A.; Yuan, J. Survey on UAV Cellular Communications: Practical Aspects, Standardization Advancements, Regulation, and Security Challenges. *IEEE Commun. Surv. Tutor.* **2019**, *21*, 3417–3442.
5. Amrallah, A.; Mohamed, E.M.; Tran, G.K.; Sakaguchi, K. UAV Trajectory Optimization in a Post-Disaster Area Using Dual Energy-Aware Bandits. *Sensors* **2023**, *23*, 1402.
6. Amrallah, A.; Mahmoud, M.E.; Khanh, T.G.; Sakaguchi, K. Optimization of UAV 3D trajectory in a post-disaster area using dual energy-aware bandits. *IEICE Commun. Express* **2023**, *12*, 403–408.
7. Mohamed, E.M.; Hashima, S.; Hatano, K. Energy Aware Multiarmed Bandit for Millimeter Wave-Based UAV Mounted RIS Networks. *IEEE Wirel. Commun. Lett.* **2022**, *11*, 1293–1297.
8. Mohamed, E.M.; Alnakhli, M.; Hashima, S.; Abdel-Nasser, M. Distribution of Multi MmWave UAV Mounted RIS Using Budget Constraint Multi-Player MAB. *Electronics* **2023**, *12*, 12.
9. Jin, H.; Jin, X.; Zhou, Y.; Guo, P.; Ren, J.; Yao, J.; Zhang, S. A survey of energy efficient methods for UAV communication. *Veh. Commun.* **2023**, *41*, 100594.
10. Alsamhi, S.H.; Ma, O.; Ansari, M.S. Survey on artificial intelligence based techniques for emerging robotic communication. *Telecommun. Syst.* **2019**, *72*, 483–503.
11. Ju, Y.; Cao, Z.; Chen, Y.; Liu, L.; Pei, Q.; Mumtaz, S.; Dong, M.; Guizani, M. NOMA-Assisted Secure Offloading for Vehicular Edge Computing Networks with Asynchronous Deep Reinforcement Learning. *IEEE Trans. Intell. Transp. Syst.* **2023**, 1–14.
12. Song, H.; Bai, J.; Yi, Y.; Wu, J.; Liu, L. Artificial Intelligence Enabled Internet of Things: Network Architecture and Spectrum Access. *IEEE Comput. Intell. Mag.* **2020**, *15*, 44–51.
13. Hammouti, H.E.; Hamza, D.; Shihada, B.; Alouini, M.S.; Shamma, J.S. The Optimal and the Greedy: Drone Association and Positioning Schemes for Internet of UAVs. *IEEE Internet Things J.* **2021**, *8*, 14066–14079.
14. Bai, C.; Yan, P.; Yu, X.; Guo, J. Learning-based resilience guarantee for multi-UAV collaborative QoS management. *Pattern Recognit.* **2021**, *122*, 108166.
15. Han, S.I. Survey on UAV Deployment and Trajectory in Wireless Communication Networks: Applications and Challenges. *Information* **2022**, *13*, 389.
16. Shakhathreh, M.; Shakhathreh, H.; Ababneh, A.A. Efficient 3D Positioning of UAVs and User Association Based on Hybrid PSO-K-Means Clustering Algorithm in Future Wireless Networks. *Mobile Information Systems* **2023**, *2023*, 6567897.
17. Siddiqui, A.B.; Aqeel, I.; Alkhayyat, A.; Javed, U.; Kaleem, Z. Prioritized User Association for Sum-Rate Maximization in UAV-Assisted Emergency Communication: A Reinforcement Learning Approach. *Drones* **2022**, *6*, 45.
18. Xi, X.; Cao, X.; Yang, P.; Chen, J.; Quek, T.; Wu, D. Joint User Association and UAV Location Optimization for UAV-Aided Communications. *IEEE Wirel. Commun. Lett.* **2019**, *8*, 1688–1691.
19. El Hammouti, H.; Benjillali, M.; Shihada, B.; Alouini, M.S. Learn-As-You-Fly: A Distributed Algorithm for Joint 3D Placement and User Association in Multi-UAVs Networks. *IEEE Trans. Wirel. Commun.* **2019**, *18*, 5831–5844.
20. Cheng, F.; Zou, D.; Liu, J.; Wang, J.; Zhao, N. Learning-Based User Association for Dual-UAV Enabled Wireless Networks With D2D Connections. *IEEE Access* **2019**, *7*, 30672–30682.
21. Sun, Y.; Wang, T.; Wang, S. Location Optimization and User Association For Unmanned Aerial Vehicles Assisted Mobile Networks. *IEEE Trans. Veh. Technol.* **2019**, *68*, 10056–10065.
22. Yin, S.; Li, L.; Yu, F.R. Resource Allocation and Basestation Placement in Downlink Cellular Networks Assisted by Multiple Wireless Powered UAVs. *IEEE Trans. Veh. Technol.* **2020**, *69*, 2171–2184.
23. Plachy, J.; Becvar, Z.; Mach, P.; Marik, R.; Vondra, M. Joint Positioning of Flying Base Stations and Association of Users: Evolutionary-Based Approach. *IEEE Access* **2019**, *7*, 11454–11463.
24. Qiu, C.; Wei, Z.; Yuan, X.; Feng, Z.; Zhang, P. Multiple UAV-Mounted Base Station Placement and User Association With Joint Fronthaul and Backhaul Optimization. *IEEE Trans. Commun.* **2020**, *68*, 5864–5877.
25. Yu, C.S. Graph theory, by W. T. Tutte, Encyclopedia of Mathematics and its Applications, Volume 21, Addison-Wesley Publishing Company, Menlo Park, CA, 1984, 333 pp. Price: 45.00. *Networks* **1986**, *16*, 107–108.
26. Hande, P.; Rangan, S.; Chiang, M.; Wu, X. Distributed Uplink Power Control for Optimal SIR Assignment in Cellular Data Networks. *IEEE/ACM Trans. Netw.* **2008**, *16*, 1420–1433.
27. Chen, Y.; Wong, W.S. Power control for non-Gaussian interference. In Proceedings of the 7th International Symposium on Modeling and Optimization in Mobile, Ad Hoc, and Wireless Networks, Seoul, Korea, 23–27 June 2009; pp. 1–8.
28. Masroor, R.; Naeem, M.; Ejaz, W. Resource management in UAV-assisted wireless networks: An optimization perspective. *J. Netw. Comput. Appl.* **2022**, *205*, 103439.

29. Zeng, Y.; Zhang, R.; Lim, T.J. Wireless communications with unmanned aerial vehicles: Opportunities and challenges. *IEEE Commun. Mag.* **2016**, *54*, 36–42.
30. Alnakhli, M.; Anand, S.; Chandramouli, R. Joint Spectrum and Energy Efficiency in Device to Device Communication Enabled Wireless Networks. *IEEE Trans. Cogn. Commun. Netw.* **2017**, *3*, 217–225.
31. Poole, G.D.; Boullion, T.L. A Survey on M-Matrices. *Siam Rev.* **1974**, *16*, 419–427.
32. Meyer, C.D. *Matrix Analysis and Applied Linear Algebra*; SIAM: Philadelphia, PA, USA, 2000.

Disclaimer/Publisher’s Note: The statements, opinions and data contained in all publications are solely those of the individual author(s) and contributor(s) and not of MDPI and/or the editor(s). MDPI and/or the editor(s) disclaim responsibility for any injury to people or property resulting from any ideas, methods, instructions or products referred to in the content.